JOURNAL OF MATERIALS SCIENCE 28 (1993) 811–816

Preparation and properties of ZnS thin films by low-pressure metalorganic chemical vapour deposition

C. H. LEE, C. Y. PUENG
Graduate Institute of Materials Engineering, Cheng Kung University, Tainan, Taiwan

Low-pressure metalorganic chemical vapour deposition of ZnS thin films on silicon, oxidized silicon and glass substrates using Zn $(C_2H_5)_2$ and C_4H_4S as source chemicals was investigated. The growth process and the film properties were characterized as functions of process parameters including substrate temperature, reactant ratio and reaction pressure. In general, growth rates as a function of substrate temperature were found to reach a maximum at a much lower temperature than that for growth at atmospheric pressure. In addition, growth rates increased with reaction pressure and thiophene flow rate depending on the temperature condition. The microstructure indicated that growths above 250 °C possess a cubic (zincblende) structure, while growths below 150 °C are polycrystalline of wurtzite structure. The resistivity varies from 10^4 Ω cm to a maximum of about 3×10^5 Ω cm for growth at 250 °C, depending on the reactant ratio. The details are discussed in the text.

1. Introduction

For many years ZnS has been of great interest for optoelectronic development as a potential light-emitting material for colour display systems [1, 2] because it possesses excellent luminescent properties and has a wide band gap which covers all the visible spectrum. However, thin-film electroluminescent ZnS devices have only been extensively investigated in recent years for flat panel display application [3–7]. Because the requirements of thin-film devices are to have low threshold voltage and high luminescent efficiency, investigations on ZnS thin films have focused on the problems of threshold voltage reduction and emission efficiency enhancement [7–13].

In general, the threshold voltage and luminescent efficiency of the devices are very different not only due to the preparation process and doping conditions but also depending on the device processing history. Of course, device structures and properties of the dielectric window material can also lead to a different luminescent condition. In short, the data of luminescent properties of ZnS thin films are scattered with a wide range of threshold voltages from 10–100 V and of efficiencies from 0.1%–10%. No investigators appear to be sure about the exact luminscent and reliability mechanisms of the thin-film devices. However, most have found that light emission originates from the activator dopants in the grain lattice of good crystallinity and the efficiency can be improved by heat treatment of the thin films prior to device fabrication.

ZnS crystallizes into zincblende structure while it transforms to wurtzite structure at temperatures higher than 1300 °C. Although it has a high melting point of about 1830 °C, it is physically not very stable at temperatures above 500 °C, because of high vapour pressures of sulphur and zinc. However, crystallization of ZnS easily takes place, because it is a strongly ionic bonding compound. Therefore, crystalline ZnS thin films can readily be prepared by various means at low temperatures on different substrates. The techniques which have been investigated for ZnS synthesis include reactive evaporation [14, 15], sputtering [16, 17], metalorganic chemical vapour deposition [MOCVD] [18–22] and MBE [23, 24]. Because MOCVD has been considered to possess high potential for growth of quality crystalline thin films of device grade in quantity, this work was initiated to use organosulphur of high decomposition temperature, C_4H_4S, and $Zn(C_2H_5)_2$ as source chemicals to deposit ZnS thin films on substrates of different kinds in an attempt to improve the film quality to reduce the threshold voltage and to enhance the luminescent efficiency.

2. Experimental procedure

In this work, ZnS MOCVD was carried out at a reduced pressure of 10–50 torr (1 torr = 133.322 Pa) in a home-made reaction system which is schematically shown in Fig. 1. Briefly, it consists of three sections of apparatus which include a quartz reaction tube with an insulated resistance-heated pedestal, a gas manifold with mass flowmeters, a pressure sensor and a hydrogen purifier, and a mechanical pump connected to four scrubbing tanks for exhausting

0022–2461 © 1993 Chapman & Hall

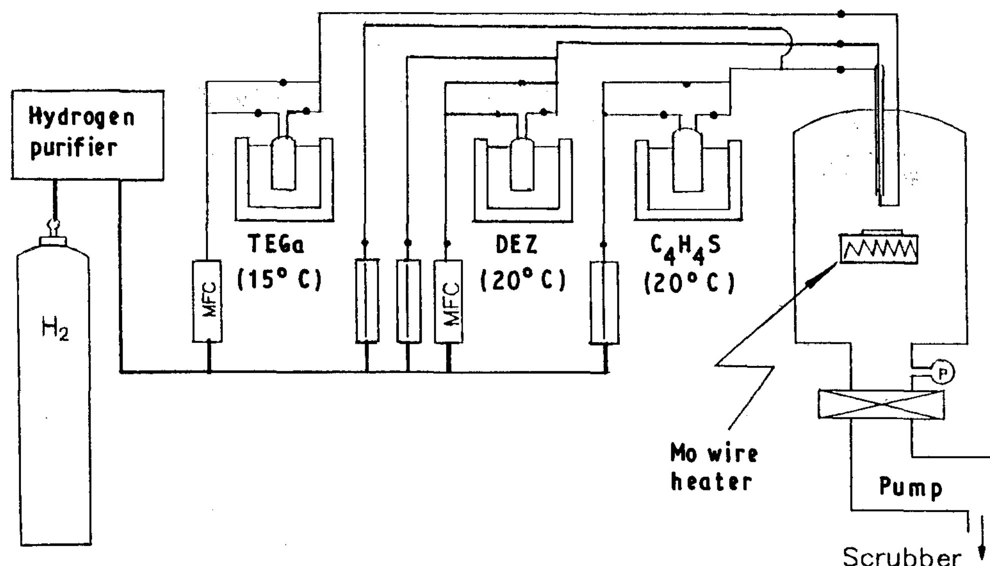

Figure 1 Schematic drawing of the MOCVD apparatus. MFC, mass flow controller; TEGA.

gases. Thiophene and diethylzinc (DEZ) were used as reactants which were kept at 20 °C. Hydrogen was used as a carrier gas. IC grade (1 0 0)Si wafers of 1–5 Ω cm resistivity, and oxidized silicon wafers with about 100 nm SiO_2 were mainly used as substrates for process investigation, while for electroluminescent device study, an additional layer of conductive material was deposited on the regular substrates. The deposition temperatures were between 150 and 300 °C. The reaction chamber pressure was kept constant between 10 and 50 torr, while the total gas flow rate through the chamber was fixed between 0.5 and 1 l/min.

The growth characteristics of ZnS thin films were analysed by ellipsometry measurement of the film thickness and refractive index. The microstructure and surface morphology were determined by X-ray, TEM and SEM analysis. The chemical composition and completeness of reaction were characterized using Auger electron spectroscopy (AES) and Fourier transform infrared (FTIR) analysis. The ratio of zinc to sulphur in the solid phase was determined from energy dispersive X-ray analysis (EDX) peak intensity measurement.

For characterization of electrical and electroluminescent properties, the Al/ZnS/Si and Al/InO_x/GaN–ZnS–GaN/InO_x/Si device structures were fabricated by spray pyrolysis deposition of InO_x and electron-beam evaporation of aluminium. The devices were subjected to a brief heat treatment of about 30 min at 400 °C in a forming gas (N_2 + 15%H_2) atmosphere. *CV* and *IV* measurements were carried out using two sets of standard equipment. The electroluminescent properties were analysed using a spectrometer in the visible range; the detailed results will be published elsewhere.

3. Results and discussion

For ZnS thin-film deposition, most of the MOCVD experiments used H_2S as a sulphur source to react with $Zn(C_2H_5)_2$ under atmospheric pressure. Because of the nature of the reactants, the reaction takes place readily in the chamber before reaching the substrate surface. This usually leads to a homogeneous reaction resulting in particulate inclusions and crystalline defects. However, C_4H_4S is a more stable sulphur compound. It has been used for ZnS MOCVD under atmospheric conditions [18] and it was found that a substrate temperature higher than 400 °C was required to obtain growth of crystalline films. For the present work it was decided to use C_2H_4S with DEZ to carry out MOCVD at a reduced pressure of about 50 torr. It was expected that the growth temperature could be reduced and the doping conditions improved. In this case, trimethyl gallium was used as a dopant source which was also carried over into the reactor by hydrogen.

In order to obtain the optimum conditions for growth of high-quality thin films, the effects of important process parameters were investigated. Fig. 2 shows the effects of substrate temperature on growth rate at a fixed reaction pressure, S/Zn ratio and total flow rate with minor variations of reactant concentration as indicated. The data show an increased trend of growth rate with temperature to a maximum at 150 °C. Then it decreases as the growth rate increases. In the initial temperature range, the surface reaction mechanism is apparently growth-rate controlling, while in the higher temperature range the mass-transfer mechanism is important in controlling the growth rate. However, the decrease in growth rate with further increase in substrate temperature is due to either the decrease of sticking coefficient for adsorption or the depletion of reactants concentration near the substrate surface from volume reaction.

Fig. 3 shows the effect of pressure on growth at 250 °C with a set of fixed growth parameters. The initial growth rate increased with pressure from 20 torr to 50 torr indicating that the reaction pressure enhances the supply of reactants to the surface of the substrate where the molecules have more chance of meeting and reacting, resulting in increased growth

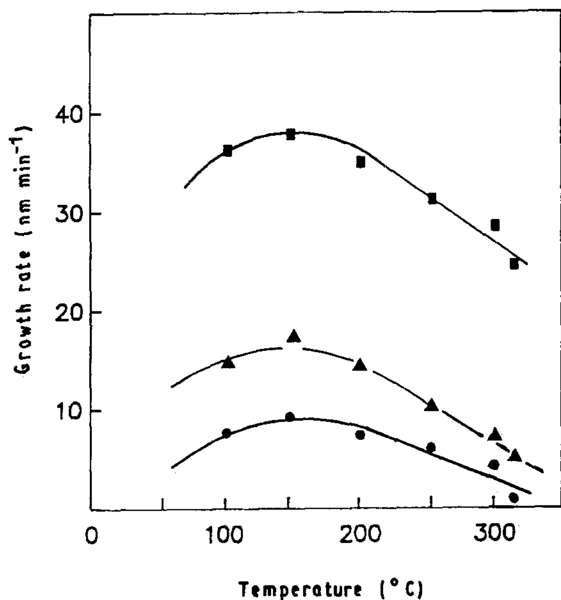

Figure 2 Growth rate versus substrate temperature. (■) DEZ flow rate = 0.3 cm^3 min^{-1}, C_4H_4S flow rate = 6 cm^3 min^{-1}. (▲) DEZ flow rate = 0.15 cm^3 min^{-1}. C_4H_4S flow rate = 2 cm^3 min^{-1}. (●) DEZ flow rate = 0.1 cm^3 min^{-1}, C_4H_4S flow rate = 2 cm^3 min^{-1}. Pressure = 2 torr, total flow rate = 300 standard cm^3 min^{-1}, $[C_4H_4S]/[DEZ] = 20$.

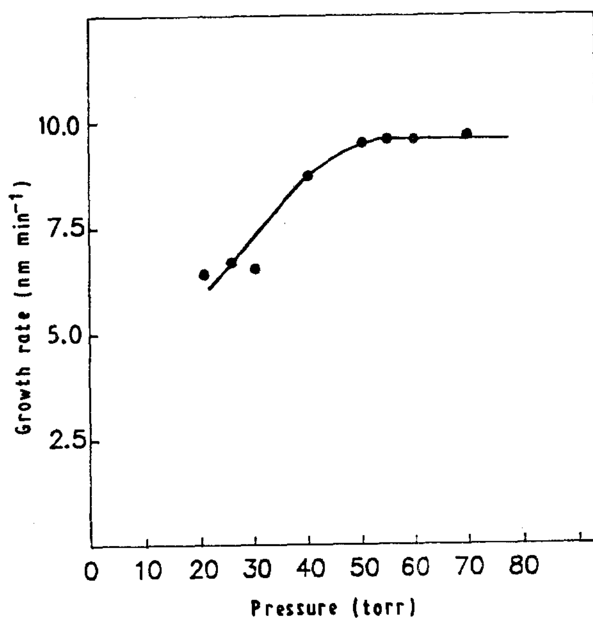

Figure 3 Growth rate versus reaction pressure. DEZ flow rate = 0.1 standard cm^3 min^{-1}, C_4H_4S flow rate = 2 standard cm^3 min^{-1}, total flow rate = 600 standard cm^3 min^{-1}. Substrate temperature = 250 °C, $[C_4H_4S/[DEZ] = 20$.

rates. However, as the pressure reaches about 50 torr, the surface reaction mechanism appears to be controlling the growth rate. Therefore, no further change in growth rate occurs as the reaction pressure increases further.

For growth at 200 °C with the C_4H_4S flow rate fixed as 2 cm^3 min^{-1}, and a total flow of 300 cm^3 min^{-1} under a reaction pressure of 2 torr, the growth rates were determined with variation of DEZ flow rate. The results are plotted in Fig. 4 which clearly indicates that

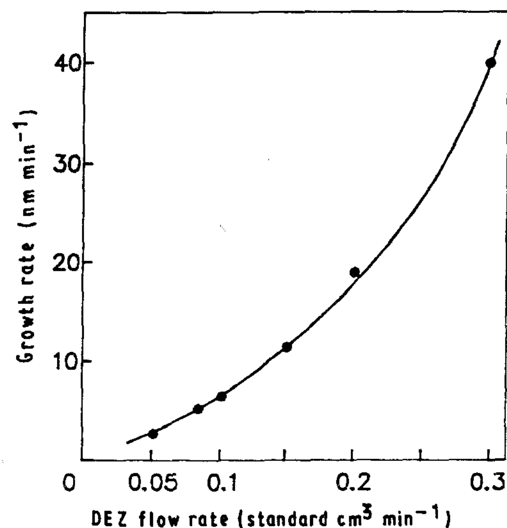

Figure 4 Growth rate versus DEZ flow rate. Pressure = 2 torr, total flow rate = 300 standard cm^3 min^{-1}, temperature = 200 °C. $[C_4H_4S]$ = 2 cm^3 min^{-1}.

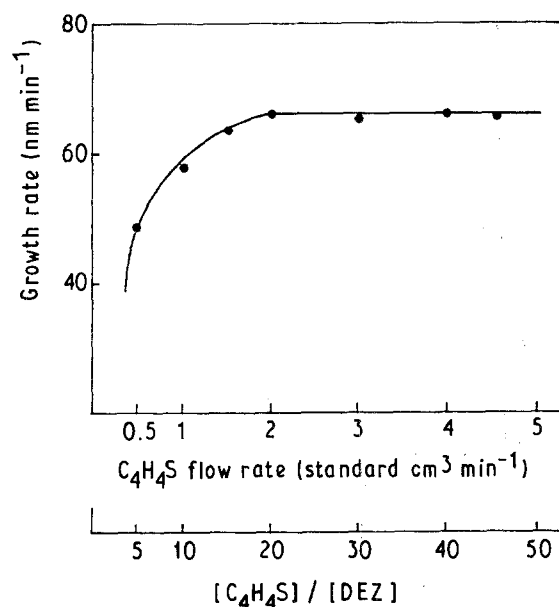

Figure 5 Growth rate versus S/Zn ratio in solid DEZ; flow rate = 0.1 standard cm^3 min^{-1}, substrate temperature = 200 °C, pressure = 2 torr, total flow rate = 300 standard cm^3 min^{-1}.

DEZ concentration predominately controls the growth rate. However, in the initial stage with very low concentration of DEZ, the growth rate increases very slowly. This means that a minimum flow rate of DEZ is needed for system compensation under the growth conditions used.

Fig. 5 shows the effect of S/Zn ratio on growth rates while the DEZ flow rate is fixed at 0.1cm^3 min^{-1}. The results indicate that a S/Zn ratio of 20 or higher is required for growth of stoichiometric ZnS, because the vapour pressure of sulphur is much higher than that of zinc. Fig. 6 shows that the film thickness is nearly linearly related to growth time, except that in the very early stage due to growth system compensation, the thickness increases very slowly. The linear relation between thickness and growth time indicates that the growth conditions are stable and reproducible.

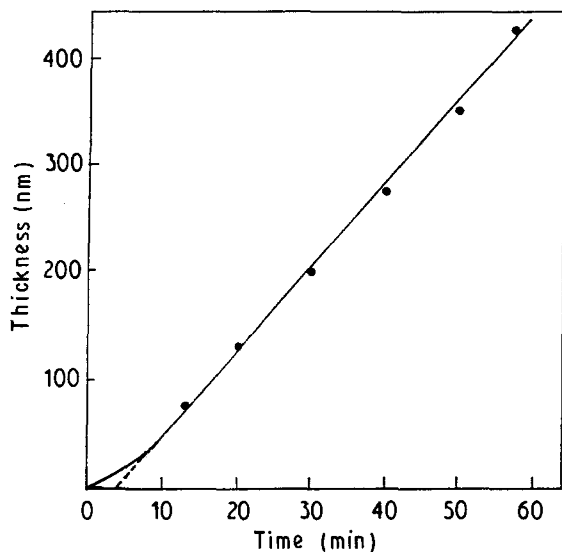

Figure 6 Film thickness versus growth time. Substrate temperature = 200 °C, $[C_4H_4S]/[DEZ] = 20$, pressure = 2 torr.

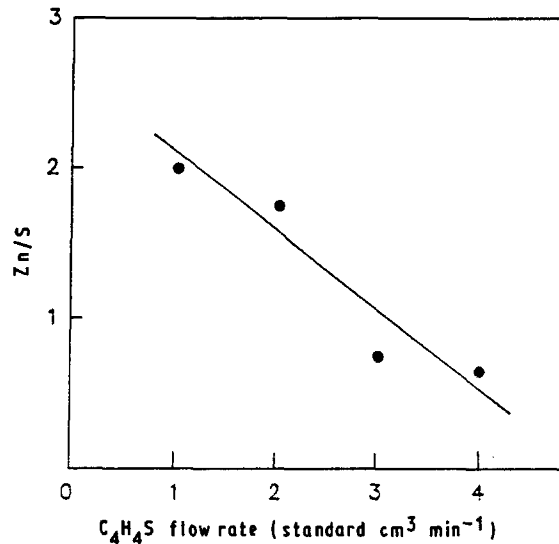

Figure 8 Solid-phase S/Zn ratio versus C_4H_4S flow rate. Substrate temperature = 250 °C, DEZ flow rate = 0.15 standard cm^3 min^{-1}, total flow rate = 300 standard cm^3 min^{-1}.

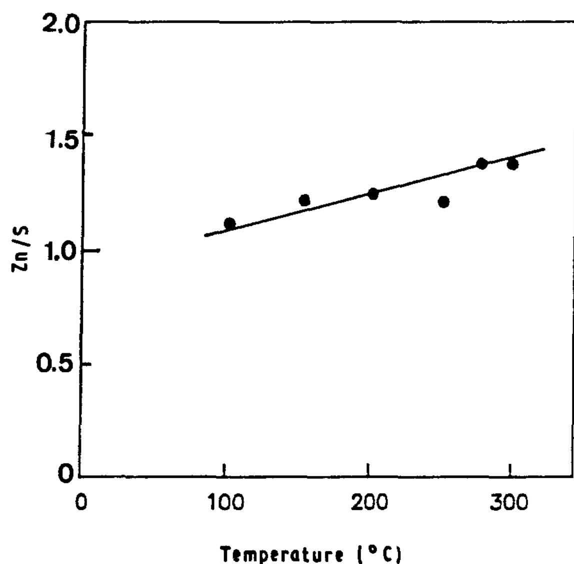

Figure 7 Solid phase S/Zn ratio versus growth temperature. DEZ flow rate = 0.1 standard cm^3 min^{-1}, C_4H_4S flow rate = 2.5 standard cm^3 min^{-1}, total flow rate = 300 standard cm^3 min^{-1}.

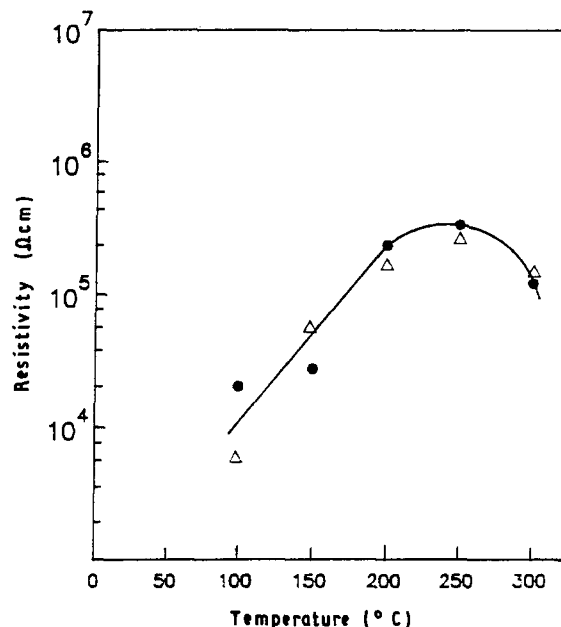

Figure 9 Resistivity versus growth temperature in undoped ZnS (400 nm). (●) I–V test, Al/ZnS/n-Si structure, (△) four-point probe measurement.

Auger electron spectroscopy analysis was used for composition determination. The results of Zn/S ratio in the solid phase are plotted against growth temperature in Fig. 7 for samples grown with S/Zn = 25 in the gaseous phase and a fixed total flow rate of 300 cm^3 min^{-1}. The data show that at substrate temperature between 100 and 200 °C, the composition remains nearly the same of about the stoichiometric condition of Zn/S = 1, while for growth at higher temperatures, Zn/S deviates more from 1. This is apparently caused by a fast increase of vapour pressure of sulphur at higher temperatures where a greater flow rate of C_4H_4S is needed for stoichiometric growth. Fig. 8 shows solid-phase Zn/S ratio plotted against the flow rate of C_4H_4S for growth at 250 °C. The decreasing trend verifies the data in Fig. 7. Thus the stoichiometric growth of ZnS can only be obtained at a proper temperature with a sufficiently high ratio of S/Zn in the gaseous phase.

The resistivity of the thin films was determined by measurement of the sheet resistance and film thickness. The data are plotted against the growth temperature in Fig. 9. The increase in resistivity with growth temperature for growth below 200 °C is probably due to the change in stoichiometric conditions as crystallinity improves. However, it decreases for growth above 250 °C because of defect generation due to sulphur deficiency in the crystal lattice.

Because crystallinity and structural perfection are important to light-emitting characteristics, the material aspects of microstructure of the thin films were investigated using X-ray and electron diffraction analysis. Fig. 10 shows a series of X-ray diffraction spectra

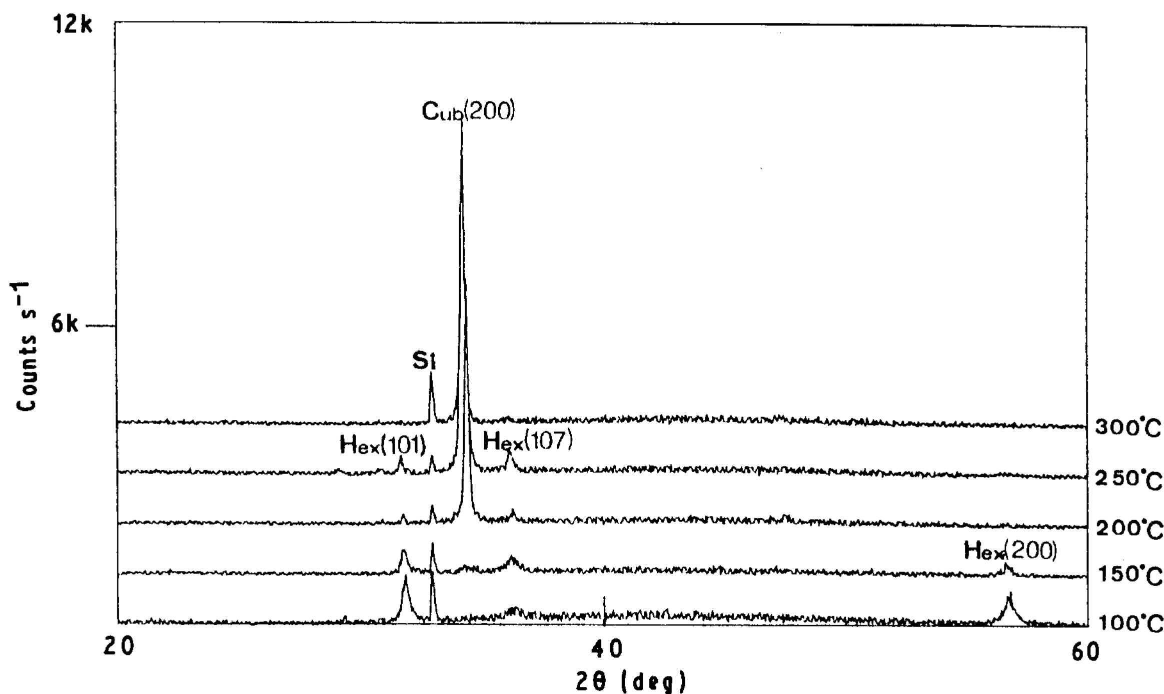

Figure 10 X-ray diffraction spectra of growths at different temperatures. $[C_4H_4S]/[DEZ] = 20$, $P = 2$ torr, total flow rate = 300 standard $cm^3\ min^{-1}$.

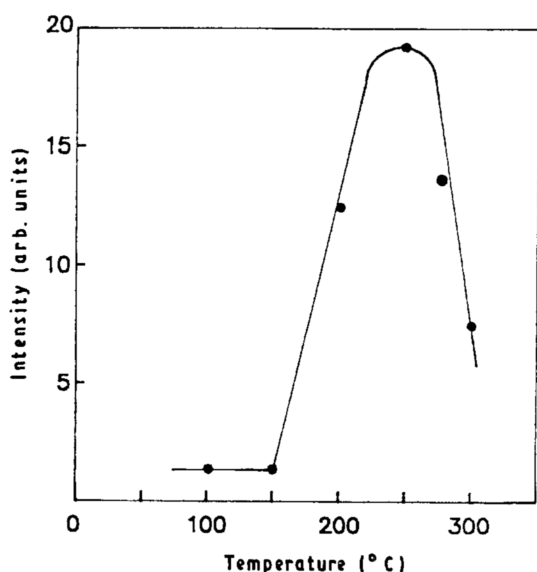

Figure 11 Cubic (2 0 0) X-ray diffraction peak intensity of unit film thickness versus growth temperature.

for the samples prepared at various substrate temperatures. The results indicate very clearly that for growth at 100 and 150 °C the spectra show diffraction peaks of (2 0 – 0) and two minor peaks of ZnS wurtzite structure. On the other hand, for growth at temperatures higher than 200 °C, the spectra show stronger cubic (2 0 0) diffraction peaks while the wurtzite lattice diffraction peaks diminish. The (2 0 0) peak intensity appears to be the strongest for growth at 250 °C while it decreases with increasing growth temperature. This is probably caused by crystallinity change due to sulphur deficiency. The relation of the (2 0 0) diffraction peak intensity per unit thickness and the growth temperature is shown in Fig. 11. Electron diffraction analysis was used to verify the X-ray diffraction data: growth at temperatures above 200 °C are zincblende while those grown at temperatures below 150 °C are wurtzite. In addition, in the low-temperature growth, twins occur in the matrix of the hexagonal structure.

4. Conclusion

Low-pressure metalorganic chemical vapour deposition of ZnS thin films on silicon using C_4H_4S and $Zn(C_2H_5)_2$ as source chemicals was investigated. The properties of the thin film have been characterized. In general, growth rates as a function of substrate temperature were found to reach a maximum at 150 °C under a reduced pressure between 10 and 50 torr. This is a much lower growth temperature than that reported in the literature for growth at atmospheric pressure. In addition, growth rates increased with reaction pressure and thiophene flow rate, to approach asymptotic values depending on the temperature condition.

Growth with a reactant ratio of $S/Zn > 20$ resulted in stoichiometric ZnS. The resistivity increased with substrate temperature from $10^4\ \Omega$ cm to a maximum of about $3 \times 10^5\ \Omega$ cm for growth at 250 °C. It then decreased to 0.018 Ω cm for growth at 300 °C when gallium was introduced as a dopant at a maximum concentration of about 3.2 at %. The microstructure indicates that growths at 250 °C or above, possess a zincblende structure, while the structure becomes polycrystalline of wurtzite for growth below 200 °C. The films are highly transparent (85%) in the visible range of light waves. The band gap was determined to be 3.3 eV.

Acknowledgement

The authors acknowledge sponsorship of this work by the National Science Council.

References

1. Y. S. PARK and B. K. SHIN, in "Electroluminescence", edited by J. I. Pankove (Springer, New York, 1977) 197.
2. T. INOGUCHI, M. TAKEDA, Y. KAKIHARAAND and M. YOSHIDA, *SID Digest* (1974) 84.
3. J. E. BERNARD, M. F. MARTENS, D. C. NORTON and F. WILLIAMS, *IEEE Trans.* **ED-30** (1983) 448.
4. K. W. YANG and S. J. T. OWEN, *ibid.* **ED-30** (1983) 452.
5. R. MENN, R. J. TUETA, A. IZRAEL and M. BRAGUIER, *ibid.* **ED-30** (1983) 460.
6. R. MACH and G. O. MULLER, *J. Cryst. Growth* **88** (1988) 866.
7. R. TORNQVIST, *ibid.* **72** (1985) 538.
8. H. S. REEHAL and C. B. THOMAS, *Solid State Elect.* **29** (1986) 429.
9. T. MISHIMA, M. KONAGA and K. TAKAHASHI, *IEEE Trans.* **ED-30** (1983) 282.
10. M. I. ABDALLA, J. THOMAS, A. BRENAC and J. NOBLANC, *ibid.* **ED-28** (1981) 694.
11. K. OKAMOTO, Y. NASU and Y. HAMAKAWA, *ibid.* **ED-28** (1981) 698.
12. C. B. THOMAS, D. SAND and K. BRUNSON, *Appl. Phys. Lett.* **51** (1987) 195.
13. T. MINAMI, T. MIYATA, K. KITAMUIRA, H. NANTO and S. TAKATA, *Jpn J. Appl. Phys.* **27** (1988) L876.
14. H. KOZAWAGUCHI, J. OHWAKI, B. TSUJIYAMA and K. MURASE, *SID Digest* (1980) 126.
15. K. HIRABAYASHI and O. KOGURE, *Jpn J. Appl. Phys.* **34** (1985) 1484.
16. T. EMMA and M. MCDONOUGH, *J. Vac. Sci. Technol.* **A2** (1984) 362.
17. T. MATSUOKA, J. KUWATA, M. NISHIKAWA, Y. FUJITA, T. TOHDA and A. ABE, *Jpn J. Appl. Phys.* **27** (1988) 592.
18. P. J. WRIGHT, R. J. M. GRIFFITHS and B. COCKAYNE, *J. Cryst. Growth,* **66** (1984) 26.
19. A. YOSHIKAWA, A. SIRAI, S. YAMAGA and H. KASAI, *ibid.* **25** (1986) 673.
20. S. TAKATA, T. NINAMI, T. MIYATA and H. NANTO, *ibid.* **27** (1988) L247.
21. S. YAMAGA, A. YOSHIKA and H. KASAI, *J. Crystal Growth* **86** (1988) 252.
22. S. TAKATA, T. MINAMI, T. MIYATA and H. NANTO, *ibid.* **86** (1988) 257.
23. M. YOKOYMA, K. KASHIRO and S. OHTA, *Appl. Phys. Lett.* **49** (1986) 411.
24. M. KITAGAWA, Y. TOMOMURA, A. SUZUKI and S. NAKAJMA, *J. Crystal Growth* **101** (1990) 52.

Received 16 December 1991
and accepted 17 June 1992.